Integral Role of Platelet-Derived Growth Factor in Mediating Transforming Growth Factor-β1–Dependent Mesenchymal Stem Cell Stiffening

Deepraj Ghosh,[1] Loukia Lili,[2,3] Daniel J. McGrail,[1] Lilya V. Matyunina,[2,3]
John F. McDonald,[2–4] and Michelle R. Dawson[1,4]

Mesenchymal stem cells (MSCs) play an important role in matrix remodeling, fibroblast activation, angiogenesis, and immunomodulation and are an integral part of fibrovascular networks that form in developing tissues and tumors. The engraftment and function of MSCs in tissue niches is regulated by a multitude of soluble proteins. Transforming growth factor-β1 (TGF-β1) and platelet-derived growth factor-BB (PDGF) have previously been recognized for their role in MSC biology; thus, we sought to investigate their function in mediating MSC mechanics and matrix interactions. Cytoskeletal organization, characterized by cell elongation, stress fiber formation, and condensation of actin and microtubules, was dramatically affected by TGF-β1, individually and in combination with PDGF. The intracellular mechanical response to these stimuli was measured with particle tracking microrheology. MSCs stiffened in response to TGF-β1 (their elastic moduli was ninefold higher than control cells), a result that was enhanced by the addition of PDGF (100-fold change). Blocking TGF-β1 or PDGF signaling with inhibitors SB-505124 or JNJ-10198409, respectively, reversed soluble-factor-induced stiffening, indicating that crosstalk between these two pathways is essential for stiffening response. A genome-wide microarray analysis revealed TGF-β1-dependent regulation of cytoskeletal actin-binding protein genes. Actin crosslinking and bundling protein genes, which regulate cytosolic rheology through changes in semiflexible actin polymer meshwork, were upregulated with TGF-β1 treatment. TGF-β1 alone and in combination with PDGF also amplified surface integrin expression and adhesivity of MSCs with extracellular matrix proteins. These findings will provide a more mechanistic insight for modeling tissue-level rigidity in fibrotic tissues and tumors.

Introduction

MESENCHYMAL STEM CELLS (MSCs) are multipotent progenitor cells that play a critical role in tissue regeneration [1,2]. They reside in bone marrow and connective tissues [3] and differentiate into multiple cell types [4] required for tissue maintenance and repair [5]. Due to their regenerative ability, immunosuppressive nature, and capacity to secrete chemotactic factors and extracellular matrix (ECM) proteins [6,7], MSCs have been used as therapeutics in numerous applications, including myocardial infarction [8], diabetes [9], sepsis [10], lung disease [11], and wound healing [12,13]. The success of MSC-based therapies depends on their ability to interact with and engraft in diseased tissues, proliferate for long-term incorporation, and function as therapeutic agents [14]. This process is regulated not only by chemical cues such as soluble factors [13], but also by physical cues [14] such as cell shape [15] and ECM rigidity [16] within the various tissue microenvironments or niches. Though a variety of soluble factors have been shown to increase MSC migration and engraftment [17,18], the complex signaling cascades responsible for this response remain poorly understood. Earlier works have shown that both murine [19] and human [18] MSCs undergo dramatic cytoskeletal stiffening in response to the cocktail of promigratory molecules released by tumor cells. The degree of stiffening was shown to be a key differentiating factor between MSCs and their less-migratory fibroblast counterparts [19,20] and even predictive of decreased MSC function in vivo [21]. Tumor-cell-conditioned media regulate MSC survival, migration, proliferation, and differentiation in a paracrine fashion or by triggering the release of other soluble factors that act through autocrine signaling pathways [20,21].

[1]Georgia Institute of Technology, School of Chemical and Biomolecular Engineering, Atlanta, Georgia.
[2]Georgia Institute of Technology, School of Biology, Atlanta, Georgia.
[3]Georgia Institute of Technology, Integrated Cancer Research Center, Atlanta, Georgia.
[4]The Petit Institute for Bioengineering and Bioscience, Georgia Institute of Technology, Atlanta, Georgia.

Both platelet-derived growth factor-BB (PDGF) and transforming growth factor-β1 (TGF-β1) are released by tumor cells and play important roles in recruiting MSCs to target sites and influencing their growth and regenerative capacity [22–24].

TGF-β1, a secreted protein of the TGF-β superfamily, plays a critical role in embryonic development and tissue homeostasis by regulating cell proliferation, differentiation, adhesion, migration, and apoptosis [25,26]. TGF-β1 binds with high affinity to TGF-β receptor type II where it recruits TGF-β receptor type I (ALK5) to form a tetrameric signaling complex [27]. Upon activation, TGF-β1 signaling pathways influence a myriad of cell processes through SMAD-dependent or independent pathways [27]. Abnormalities in TGF-β signaling contribute to tumor formation, cancer progression, inflammation, hypertrophic scar formation, and fibrosis [26,28,29]. The function of TGF-β1 on a cellular level is dependent on the developmental cell lineage, context of the interaction, and concentration [30]. TGF-β1 also plays an important role in remodeling cell microenvironments in the tumor or the wound bed by promoting fibroblast activation, angiogenesis, and immunomodulation [31,32]. The variation in TGF-β1-induced responses is easily illustrated in the context of cancer where TGF-β1 suppresses early tumor growth but promotes tumor progression and metastasis at later stages [33]. MSC differentiation into carcinoma-associated fibroblasts is largely influenced by TGF-β1 [34]. Inhibition of TGF-β signaling has been investigated as a treatment for immune disorders [35], fibrosis, and metastatic cancer [36].

PDGF is a key regulator of MSC growth, proliferation, survival, and chemotaxis [37,38] and is essential for MSC recruitment to nascent vessels and maturation into perivascular cells [39]. PDGF interacts with PDGFR alpha (α) and beta (β) tyrosine kinase receptors that dimerize for activation of intracellular signaling. The PDGF-B ligand interacts with both PDGFR-α and -β but PDGF-A has a higher affinity for PDGFR-α [40]. The PDGF-A/PDGFRα signaling axis is vital for proliferation and lineage commitment of mesenchymal progenitor cells during embryogenesis and organogenesis [41]. After development, MSCs primarily express PDGFR-β [42], which, with its ligand PDGF-B, plays a critical role in mediating the tropism and differentiation during vascular remodeling [41]. In addition to these paracrine signaling processes, autocrine signaling is also important in the tumor environment where it has been implicated in epithelial-to-mesenchymal transition of carcinoma cells [43].

The mechanical response of a cell to chemical or physical stimuli is critical for a multitude of cellular processes, including cell adhesion and motility, cell growth and differentiation, protein and DNA synthesis, and apoptosis. A more dynamic understanding of how mechanical stresses regulate cell functions requires increased knowledge of the microscopic mechanical properties of cells [44,45] and their extracellular environments [46]. The intracellular mechanical properties of live cells are determined by the organization of cytoskeletal actin [47,48]. Chemical and physical stimuli alter cell shape and cytoskeletal organization by activating cytoskeletal mediators, including small Rho GTPases RhoA, Rac1, and Cdc42 [15,49,50] and actin-binding proteins (ABPs), which regulate filament length through capping, branching, and severing processes [51]. ABPs may also act as linkers between actin filaments, the plasma membrane, microtubules, and intermediate filaments [51]. Actin bundling (eg, α-actinin and fascin) and crosslinking (eg, filamin) proteins give rise to actin stress fibers, which link the cell to the ECM via focal adhesion complexes [48,52,53].

This study sought to understand the mechanical and chemical responses of MSCs to TGF-β1 and PDGF-BB (referred as PDGF). MSCs interact with both these factors in many in vivo regenerative niches as well as tumor. In vitro cell mechanics studies have thus far focused on external biophysical cues [54] or combination of chemical cues to induce differentiation [55]. Examining mechanical response of MSCs to individual factors can provide better understanding of their role as stromal cells (e.g., functional role in tissue remodeling and cell recruitment) during initial stages in wound and tumor development. MSCs treated with TGF-β1 alone or in combination with PDGF exhibited dramatic elongation, condensed actin-microtubule structure, and a highly elastic cytoplasm. Although this mechanophysical response was primarily in part to TGF-β1, combination of PDGF with TGF-β1 enhanced the TGF-β1-driven changes significantly. TGF-β1 treatment also resulted in increased expression of integrins and enhanced adhesion of MSCs with different ECM proteins. Molecularly, high-throughput gene expression analysis (Affymetrix MG430 2.0) demonstrated significant gene expression changes when MSCs were treated either with TGF-β1 or the combination of TGF-β1 and PDGF. Pair-wise comparisons of the genome-wide expression profiles of treated and control cells revealed that TGF-β1 affects genes involved in cytoskeletal organization, cell adhesion and ECM remodeling, production of ABPs, and epithelial-to-mesenchymal transition (EMT).

Materials and Methods

Materials

Isocove's modified Dulbecco's medium (IMDM), Dulbecco's modified Eagle medium (DMEM), ʟ-glutamine, penicillin-streptomycin, and trypsin were purchased from Mediatech and fetal bovine serum (FBS) was purchased from Atlanta Biologicals. Recombinant human proteins TGF-β1 and PDGF-BB (referred to as PDGF) were purchased from Biolegend. Rhodamine-Phalloidin, FITC-conjugated mouse anti-α-tubulin, and Fluospheres carboxylate-modified 100-nm particles (F8801) were purchased from Invitrogen. Antibodies for flow cytometry experiments were purchased from Biolegend. All other reagents were purchased from VWR unless otherwise specified.

MSC isolation and culture

Murine MSCs were isolated from the bone marrow of 6–10-week-old adult male Balb/C mice (Charles River Laboratories) and cultured in normal growth media (IMDM media supplemented with 20% FBS, 2 mM ʟ-glutamine, 100 U/mL penicillin, and 100 U/mL streptomycin). Briefly, tibiae and femurs of the mice were extracted and crushed in FBS. Cold phosphate-buffered saline (PBS) and collagenase I (2 mg/mL) solutions were added subsequently to facilitate cell extraction from bone with minimal cell damage. Finally, the solution mixture was filtered (70-µm cell strainer) and centrifuged (1,000g for 10 min) to recover the bone marrow cell population in pellet form. Media were supplanted regularly to remove nonadherent bone marrow (BM) cell populations. Once the adherent cells reached 80–90% confluency,

the cell culture was expanded and subsequently purified using EasySep™ Mouse SCA1 Positive Selection Kit (Stem-Cell Technologies). Purified MSCs between passages 2 and 6 were used for all studies. All animal studies were approved by the Georgia Institute of Technology Animal Care and Use Committee. The OPRR Animal Welfare Assurance number is A3822-01.

Soluble factor treatment

Soluble factor dilutions were created in serum-free DMEM immediately before use. Measured values of serum and plasma PDGF-BB and TGF-β1 concentrations in mice and humans vary from 0.1 to 100 ng/mL [56–60], with the majority of these values being in the range of 1–10 ng/mL. This concentration range of PDGF-BB and TGF-β1 has been used in numerous in vitro cell studies [61,62]; after screening the cell response across this concentration range, 5 ng/mL of PDGF-BB and TGF-β1 was used in our study. All experiments were carried out with four conditions: serum-free control media, 5 ng/mL PDGF, 5 ng/mL TGF-β1, and combination of PDGF and TGF-β1—each 5 ng/mL. MSCs were treated for 24 h unless otherwise specified.

Flow cytometry

MSCs were analyzed with a BD LSR-II flow cytometer to capture the effects of soluble factor treatment on cell surface markers. Briefly, both treated and untreated cells were detached from 10-cm dishes, centrifuged, and suspended in 100 μL cold FACS buffer (2% FBS and 1 mM ethylenediaminetetraaceticacid in PBS). Cells were then incubated with one of the following anti-mouse antibody panels (dilutions in parentheses): (1) PerCP-CD45 (1:100), PE-Sca1 (1:100), and APC-CD11b (1:100); (2) PE-CD51 (1:20), FITC-CD29 (1:100), and AF-647-MVCAM1/CD106 (1:200); and (3) APC-CD140b/PDGFR-β (1:20). To quantify PDGFR-β expression after 1 h, cells were primarily incubated with biotin-conjugated anti-mouse CD140b and subsequently stained with DyLight™ 488 streptavidin. All studies were performed in triplicate with at least $n = 50,000$ events per sample.

Morphological analysis

Cells were fixed and stained with crystal violet and imaged with stereoscopic microscope and Motic camera. Cell borders were traced manually and cell shape factors (CSFs), defined as $4 \times \pi \times \text{area}/(\text{perimeter})^2$, were determined using Image J.

Immunofluorescence staining

To visualize cytoskeletal proteins, MSCs were cultured and treated on glass cover-slips in 24-well plates. Twenty-four hours after soluble factor treatment, the actin-tubulin network was stained as previously described [19]. Cells were imaged with an inverted Zeiss LSM 510 UV confocal microscope. Nuclear elongation factor was determined by segmenting out nuclei using Otsu's method after background subtraction, and then was defined as $4 \times \pi \times A/P^2$, where A is the area of the nucleus and P is the perimeter of the nucleus. To segment out actin stress fibers, background-subtracted images were convolved with a Laplacian of

Gaussian filter to isolate fiber-like features. After segmentation, sequential image dilation and erosion using a linear structuring element with varying degrees of rotation was used to join any disconnected stress fibers and erode any small regions produced by image noise. All image analysis was performed in custom-written MATLAB algorithms [19].

Microarray data analysis

Gene expression analysis of treated and untreated MSCs was performed in triplicate using three independent replicates per condition. The Affymetrix GeneChip Mouse Genome 430 2.0 microarray chips were used for these studies. Affymetrix .CEL files were processed using Expression Console Software Version 1.1 with the Robust Microarray Analysis algorithm. The normalized expression values of each gene were $\log_2$ transformed and used for further analysis.

Unsupervised analysis. From the initial 45,101 probe sets (genes) on the Affymetrix Mouse Genome 430 2.0 chip, 42,129 displayed marginal differences in expression across all samples [standard deviation (SD) ≤0.5 from the mean of all samples] and were filtered out. The remaining 2,972 probe sets were employed in the unsupervised clustering analysis using the Spotfire Decision Site 9.1.2 (TIBCO Software: http://spotfire.tibco.com/) with the UPGMA (unweighted average) method and the Euclidean distance as the similarity measure.

Supervised analysis. From the initial 45,101 probe sets (genes) on the Affymetrix Mouse Genome 430 2.0 chip, 13,777, 19,672, and 19,618 genes displayed expression values ≥0.2 SD from the mean across the control and the cell treatments of PDGF, TGF-β1, and PDGF-TGF-β1, respectively. From these, the differentially expressed genes between each cell treatment (PDGF, TGF-β1, and PDGF–TGF-β1) and the control samples were computed using stringent false discovery rate (FDR) criteria. The significant probe sets were 842 (FDR of 1.5%), 10,617 (FDR of 2.4%), and 8,117 (FDR of 2.13%) for the PDGF, TGF-β1, and PDGF–TGF-β1, respectively. These genes were employed in pathway enrichment analyses using the GeneGO software (http://genego.com/) (Supplementary Table S1). A concise list of critically regulated genes are provided in Supplementary Table S2 (Supplementary Data are available online at www.liebertpub.com/scd).

Live-cell microrheology

Intracellular mechanical properties of living cells were determined by multiple particle tracking microrheology (MPTM), as previously described [20,21]. Briefly, 100-nm probe particles were injected into the cytosol of MSCs using PDS-1000 Biolistic Helium Particle Injection System (BioRad). The thermal motion of these probes is directly related to local rheological properties via the Stokes–Einstein equation. High spatiotemporal resolution videos of injected cells were collected with a Nikon CFI Apochromat TIRF 100×oil-immersion lens (NA = 1.49) on a Nikon Eclipse Ti inverted epifluorescent microscope maintained at 37°C and 5% carbon dioxide. A custom MPT routine incorporated in the MetaMorph software (Molecular Devices) was then used to simultaneously monitor the coordinates of 5–20 particles per video. For each condition, particles were tracked in a minimum of 10 cells per condition. Time-dependent individual particle mean square displacements (MSDs) were ensemble

averaged and used to determine the average frequency-dependent elastic moduli (G'), viscous moduli (G''), and phase angle (φ), which were reported in this study.

Centrifugal-force-based adhesion assay

This fluorometric assay was used to evaluate the effect of soluble factor treatment on MSC adhesion to native ECM, collagen, or fibronectin [21]. Briefly, MSCs were trypsinized and seeded in a 96-well plate that was coated with $10 \mu g/mL$ of desired ECM molecule or left uncoated for native ECM control ($n = 8$ wells per condition). After 24 h of treatment with soluble factors, cells were labeled with a transmembrane fluorescent viability marker, Calcein AM (Anaspec), and an initial fluorescence reading was recorded. Cells were detached by centrifuging inverted plates at $500g$ for 5 min before recording a final fluorescence reading. The adherent fraction was determined by normalizing the final florescence values with the initial prespin values.

Inhibition studies

SB-505124 and JNJ-10198409 (Sigma) were used to inhibit TGF-β1 and PDGF signaling, respectively. These chemicals bind to their corresponding cell surface receptors and block signaling pathways. Concentrations were determined from literature review and titration studies, which were used to identify maximum concentration, associated with nonsignificant viable cell loss. These initial concentration ranges have previously been used to inhibit TGF-β1-dependent migration [63] and differentiation [64] of MSCs and PDGFR-β-dependent kinase activity in NIH 3T3 [65] and proliferation in tumor cells [65,66]. For all studies, MSCs were treated with $1 \mu M$ SB-505124 and/or 50 nM JNJ-10198409 for 1 h prior to soluble factor treatment.

Gene expression analysis

RNA was isolated from treated cells using RiboZol RNA extraction reaction, and cDNA was synthesized by reverse transcription using the BioRad i-Script cDNA synthesis kit. Primers were designed using NCBI primer-blast (http://ncbi.nlm.nih.gov/tools/primer-blast/) and PrimerBank (http://pga.mgh.harvard.edu/primerbank/). All primer sequences are listed in Supplementary Table S3. Polymerase chain reaction (PCR) was carried out to amplify gene sequences as per manufacturer's recommendation for Promega PCR reaction kit. Gel electrophoresis was performed with 2% (w/v) agarose gel to visualize amplified DNA. All values are normalized to endogenous control *18sRNA*. For quantitative real-time PCR analysis of Rho-GTPases, target sequences were amplified using SsoAdvanced SYBR Green Supermix (BioRad) in an AB Step One Plus thermocycler (Applied Biosystems). All values are reported relative to control after normalization to endogenous control *GAPDH*.

Statistics

Each experiment was performed with three or more replicates, and all values are expressed as the mean ± standard error of the mean. One-way analysis of variance (ANOVA) test with repeated measures was used to determine statistical significance of experiments involving four groups. For comparison between groups, Tukey's HSD post-test was used. Significance was reported as *(for $P < 0.05$), **(for $P < 0.005$), and ***(for $P < 0.0005$). A detailed output from post-hoc analyses are provided in Supplementary Table S4.

Results

MSCs respond mechanically to TGF-β1 and PDGF treatment

MPTM was used to characterize the mechanical response of MSCs to soluble factors. For these studies, the intracellular rheology was characterized from the MSDs of 100-nm probe particles embedded in the cytoplasm (Fig. 1). In control MSCs, particle MSDs varied linearly with time (Fig. 1A), demonstrating the viscous nature of the MSC cytoplasm [19], which corresponded with viscous moduli (G'') that were higher than the elastic moduli (G') for all frequencies (Fig. 1B). After treatment with PDGF (5 ng/mL), the majority of particle MSDs still varied linearly with time, indicating that the cytosol remained primarily viscous. Further, the average viscous and elastic moduli of PDGF-treated cells were similar to control, although a small population of particles ($\sim 5\%$) encountered a more elastic cytoplasm. Treatment with an equivalent amount of TGF-β1 resulted in a homogeneous particle transport response, with 100% of the embedded particles encountering a more elastic cytoplasm as evident by particle MSDs independent of time and corresponding elastic moduli higher than the viscous moduli for all frequencies. This homogeneous stiffening response was also seen in cells treated with PDGF and TGF-β1; however, combination treatment resulted in sixfold lower MSDs compared with TGF-β1 at $\tau = 1 s$ ($P < 0.05$). At the corresponding frequency, the average elastic moduli of MSCs treated for 24 h with TGF-β1 and the combination of PDGF and TGF-β1 was 9-fold and 100-fold greater than control ($P < 0.05$), respectively. Further comparison of viscoelastic properties using phase angle indicates that control and PDGF-treated cells remain primarily viscous as φ remains $> 45°$ whereas for TGF-β1-treated cells individually and in combination with PDGF display phase angle well below 45°, indicating severe cytosolic stiffening (Fig. 1D).

Since previous work has shown that MSC shape can contribute to cell stiffness [67], we stained the cells after 24 h with crystal violet to analyze cell morphology. In good agreement with the previous work, dramatic cell elongation was associated with TGF-β1 treatment, both individually and in combination with PDGF (Fig. 1C). The morphological changes were more quantitatively assessed using a CSF that varies from 0 for a line to 1 for a perfect circle. The CSF decreased significantly ($P < 0.0005$) in response to TGF-β1 treatment alone and in combination with PDGF, indicating that cells had elongated in response to these treatments (Fig. 1E). Interestingly, PDGF alone did not alter cell morphology; however, it significantly ($P < 0.0005$) enhanced the elongation effects of TGF-β1.

TGF-β1 alters cytoskeletal organization of MSCs

Next, changes in cytoskeletal organization involved in modifications in cell stiffness and elongation were examined with immunofluorescence staining of microtubules (green),
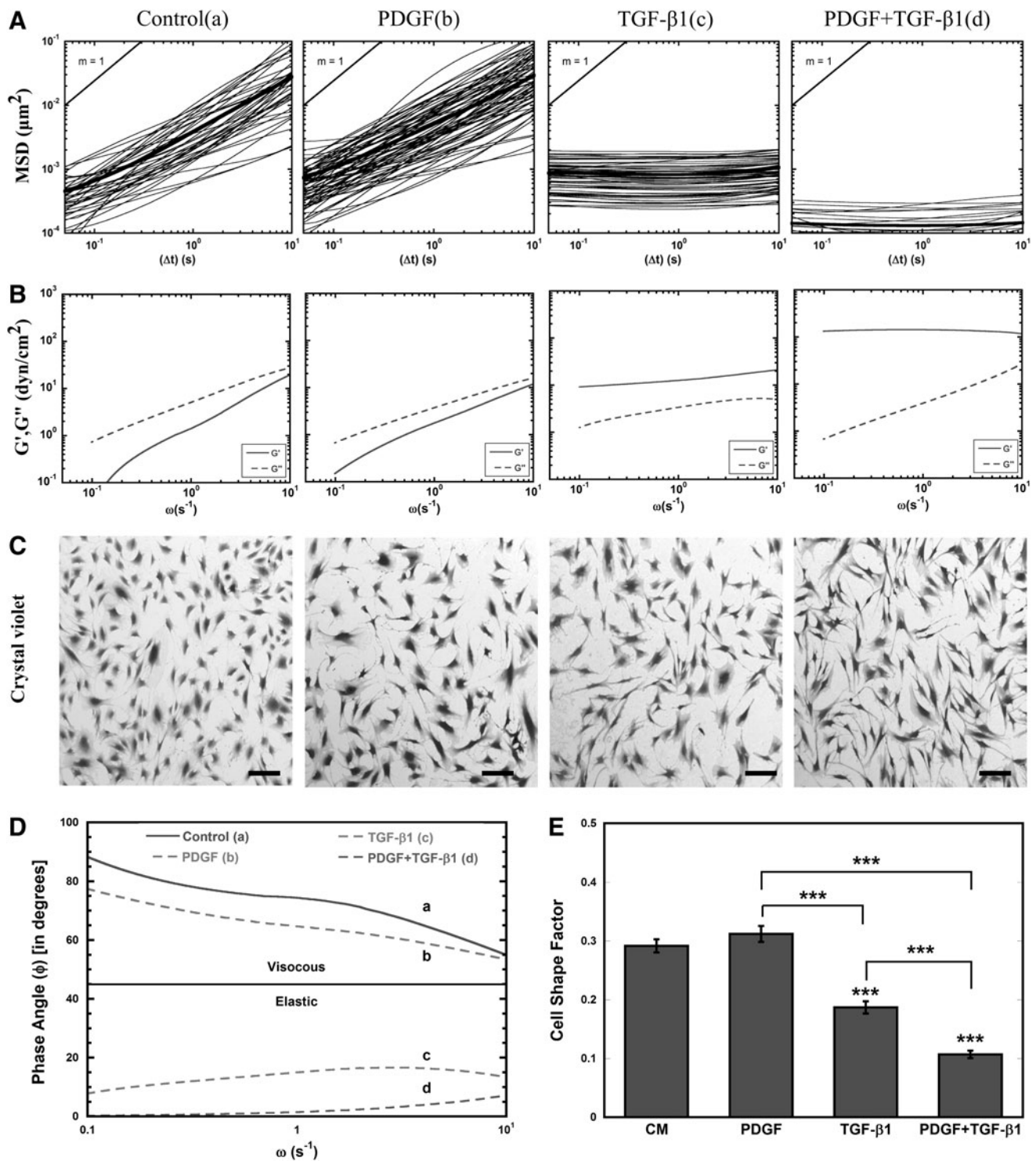
FIG. 1. Transforming growth factor-β1 (TGF-β1) alters rheology of mesenchymal stem cell (MSC) cytosol. **(A)** The ensemble averaged mean squared displacements (MSDs) of 100-nm particles embedded in the cytoplasm of murine MSCs (isolated from Balb/C mouse bone marrow) incubated for 24 h in control media [CM (a)], 5 ng/mL PDGF (b), 5 ng/mL TGF-β1 (c), and combination of PDGF and TGF-β1—each 5 ng/mL [PDGF + TGF-β1 (d)]. **(B)** The time-dependent ensemble averaged MSDs of 100-nm particles embedded in the cytoplasm of MSCs were converted to frequency-dependent elastic (G') and viscous (G'') moduli using a custom-written algorithm for Matlab software. **(C)** Brightfield images for soluble-factor-treated MSCs [conditions (a–d)] after 24 h stained with crystal violet. MSCs elongated dramatically in response to TGF-β1 individually and in combination with PDGF, whereas MSCs did not respond to PDGF treatment alone (scale bar = 100 μm). **(D)** Phase angle (φ in degrees) proportional to the ratio of viscous to elastic modulus was calculated using G' and G''. **(E)** Cell shape factor (CSF) was determined by analysis of brightfield images with image J. CSF was used to characterize the elongation of the cell, with a shape factor of 1 indicating a perfect circle and 0 indicating a straight line. Results are reported as average ± standard error of the mean (SEM, $n = 3$). Statistical significances are indicated as (*) for $p < 0.05$, (**) for $p < 0.005$, and (***) for $p < 0.0005$.

filamentous actin (red), and nuclei (blue) (Fig. 2A). Confocal images revealed condensed and elongated microtubules and actin filaments in cells treated with TGF-β1 alone or in combination with PDGF. Cells treated with TGF-β1 alone were also arranged in a parallel structure, which was somewhat disrupted in combination treatment. For combination treatment condition, the nuclear shape factor, which is the nuclear equivalent of CSF, was reduced significantly ($P < 0.0005$), indicating that nuclei had elongated (Fig. 2B), which may be required for navigating narrow pores within the ECM [19]. The actin stress fiber density, which measures the density of bundled actin filaments relative to cell area, was significantly ($P < 0.05$) higher in MSCs treated with TGF-β1 alone or in combination with PDGF (Fig. 2C).

TGF-β1 and PDGF alter MSC adhesion

Due to the dramatic rearrangement of cytoskeletal filaments, we next sought to analyze changes in the expression of the focal adhesion complexes that link the actin cytoskeleton to the extracellular environment by staining for the focal adhesion marker vinculin (Fig. 3A). Though the amount of vinculin expressed did not change significantly (Supplementary Fig. S1A), it did relocalize only to the tips of extensions in cells exposed to TGF-β1. Despite the lack of change in vinculin expression, a functional adhesion analysis with a centrifuge-based adhesion assay (Fig. 3B) revealed that MSCs treated with PDGF were significantly ($P < 0.05$) less adhesive than control cells on tissue culture plastic (TCP) (32.9%); whereas, TGF-β1-treated cells were up to 54% more adhesive than control ($P < 0.0005$). Combination treatment with PDGF and TGF-β1 also resulted in increased MSC adhesion ($P < 0.0005$) relative to control (75%), indicating that cell adhesion is largely regulated by TGF-β1. After 24 h, the adhesion of MSCs with collagen (COL) and fibronectin (FBN) was similar to TCP, since MSCs likely had sufficient time to secrete their own ECM proteins.

To reconcile these differences, flow cytometry was used to analyze differences in expression of integrin subunits β1 (CD29, Fig. 3D) and αv (CD51, Fig. 3D), which bind directly to the ECM, as well as cell adhesion molecules vascular cell adhesion molecule-1 (VCAM-1) (Fig. 3D) and intercellular adhesion molecule-1 (ICAM-1) (Supplementary Fig. S1C, D), which mediate cell–cell adhesion with endothelial cells and leukocytes. PDGF treatment had little effect on the expression of these cell adhesion molecules (CAMs), with almost no significant differences in mean fluorescence intensity (MFI, Fig. 3C) or percentage of positive cells (PPCs, Supplementary Fig. S1B) for all markers. In contrast, treatment with TGF-β1 significantly altered CAM expression as demonstrated by increased MFI and PPC for CD29 ($P < 0.005$) and CD51 ($P < 0.0005$) and reduced PPC for VCAM-1 ($P < 0.0005$) and ICAM-1 ($P < 0.05$) (Fig. 3C; Supplementary Fig. S1C, D). The altered CAM expression for TGF-β1-treated cells may explain the observed differences in adhesion and further demonstrates the important role of TGF-β1 in cell adhesion.

Both PDGF and TGF-β1 signaling is essential for cellular stiffening

TGF-β1 profoundly influenced the morphology, cytoskeletal structure, mechanical stiffness, and adhesion of MSCs.

Although the individual effects of PDGF on these aspects were not always identifiable, the addition of PDGF to TGF-β1 treatment amplified these cellular responses, indicating possible interaction between these two signaling pathways. To begin to understand this interaction, flow cytometry analysis was performed to analyze the surface expression of PDGFR-β in all four conditions (Fig. 4A–C). Though the PPC was only decreased for conditions containing PDGF (Fig. 4B), MFI was significantly ($P < 0.005$) decreased for all three treatments, indicating decreased levels of PDGFR-β available for binding (Fig. 4C). Additional studies suggest that this decrease in MFI is not due to a decrease in PDGFR-β surface expression, but increased binding of PDGF to its receptor blocking the antibody binding. Incubation with PDGF at short time scales (~ 1 h) reveals a rapid decrease in PDGFR MFI before changes in receptor levels from altered gene expression would be able to occur, suggesting that the decrease is due to increased levels of bound PDGF (Supplementary Fig. S1C–E). This result infers that cells treated with TGF-β1 alone were also experiencing increased levels of PDGF signaling.

To better elucidate the roles of PDGF and TGF-β1 signaling on mechanical stiffening, we decoupled these interactions with small-molecule inhibitors JNJ-10198409 and SB-505124 in tandem with soluble factor treatment. SB-505124 binds to intracellular domain of TGF-βR type I (ALK4, ALK5, and ALK7) and stops phosphorylation of SMADs to inhibit downstream TGF-β1 signaling [68]. JNJ-10198409 is a selective PDGFR-β kinase inhibitor, which blocks downstream PDGF signaling [69]. We chose the concentration of each inhibitor (JNJ-10198409—50 nM; SB-505124—1 μM) based on 24-h viability given a range of inhibitor concentrations. MSCs incubated for 1 h with SB-505124 prior to treatment with TGF-β1 alone or in combination with PDGF maintained their viscous cytosolic property similar to that of control MSCs (Fig. 4D). More interestingly, JNJ-10198409 incubation completely prevented both TGF-β1-induced and combination of PDGF- and TGF-β1-induced stiffening (Fig. 4D). These results suggest an integral role of the PDGFR-β signaling pathway in regulating TGF-β1-induced cell stiffening.

Expression profiling reveals distinct genes and pathways in MSCs treated with the TGF-β1, PDGF, and the combined PDGF and TGF-β1

From the initial 45,101 probe sets of the Affymetrix Mouse Genome 430 2.0 chip, any housekeeping genes and potential experimental noise were excluded by discarding all probe sets with expression variation of SD ≤0.5 among the 12 samples of cell treatments and controls. The remaining 2,972 probe sets were used for the unsupervised hierarchical clustering and initial expression pattern discovery (Fig. 5A). Unsupervised analysis showed expression profiles of TGF-β1 grouped with the combined PDGF and TGF-β1 cell treatment and did not group with the PDGF and control treatments.

To investigate further the differences between each cell treatment and control, and between treatments, we estimated the number of significantly differentially expressed probe sets. The Significance Analysis of Microarrays [70] revealed greater number of differentially expressed probe sets for TGF-β1 (10,617 probe sets of FDR 2.4% or 23.5% of
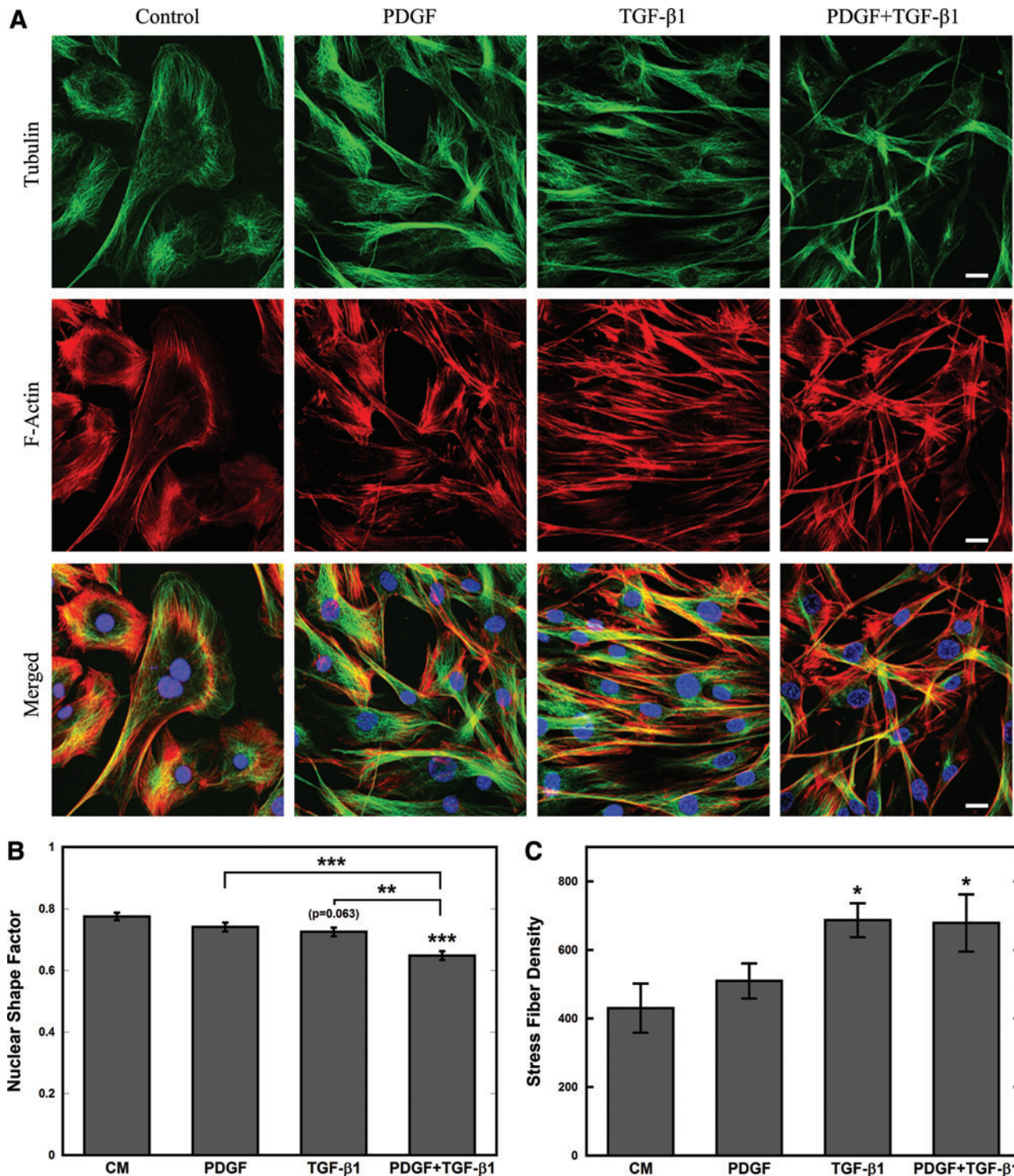
FIG. 2.   MSCs reorganize their cytoskeleton in response to TGF-β1 after 24 h. **(A)** Confocal images of soluble-factor-treated MSCs stained with Phalloidin (F-actin, *red*), anti-α-tubulin (microtubules, *green*), and 4′,6-diamidino-2-phenylindole (DAPI, nucleus, *blue*). The shape and cytoskeletal organization of CM and PDGF-treated MSCs were similar, whereas TGF-β1 with or without PDGF-treated MSCs were elongated with condensed cytoskeletal filaments (scale bar = 20 μm). **(B, C)** Cytoskeletal parameters were determined by analysis of confocal images with custom MATLAB routine. The nuclear shape factors **(B)** were used to characterize the elongation of the nucleus, respectively, with a shape factor of 1 indicating a perfect circle and 0 indicating a straight line. The stress fiber density **(C)** was used to characterize the density of actin stress fibers per cell area. Cytoskeletal changes observed in TGF-β1-treated (with or without PDGF) MSCs were confirmed using the cytoskeletal parameters, which indicated reduction in nuclear shape factor and increase in stress fiber densities. Results are reported as average ± SEM ($n = 3$). Statistical significances were indicated as (*) for $p < 0.05$, (**) for $p < 0.005$, and (***) for $p < 0.0005$. Color images available online at www.liebertpub.com/scd
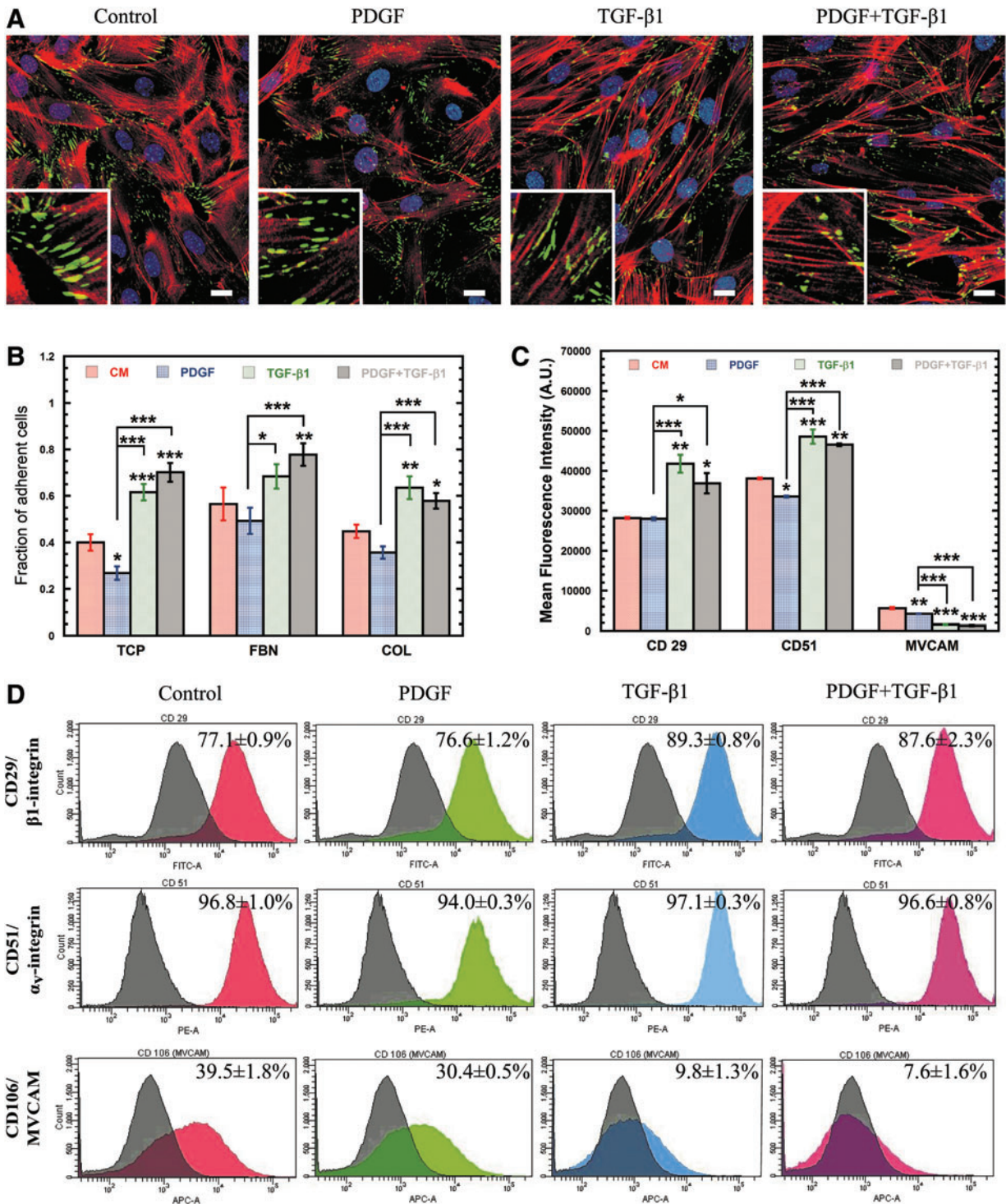
FIG. 3. Soluble factor induced changes in the strength and distribution of cell adhesion molecules (CAMs). **(A)** Confocal images of soluble-factor-treated MSCs stained with Phalloidin (F-actin, *red*), anti-vinculin (*green*), and DAPI (nucleus, *blue*) (scale bar = 20 μm). Magnified images of representative vinculin structures are shown in *insets*. **(B)** Centrifuge-based adhesion assay was used to determine the effects of soluble factor treatment on the adhesion of MSCs on tissue culture plastic coated with collagen—10 μg/ml (COL) or fibronectin—10 μg/mL (FBN). TGF-β1 treatment resulted in an increased fraction of adherent cells. Results are reported as average ± SEM ($n = 8$). **(C)** Histograms from flow cytometry were analyzed using FACS-DIVA for mean fluorescence intensity (MFI). Surface integrin expression of PDGF-treated cells was unaffected and vascular cell adhesion molecule-1 (VCAM-1) expression was slightly decreased, whereas TGF-β1 individually and in combination increased both integrin expression and reduced VCAM expression significantly compared with the control. Results are reported as average ± SEM ($n = 3$). **(D)** Histograms from flow cytometric analysis of surface CAMs using fluorescent-labeled antibodies for α_v (PE), β_1 (FITC) integrins, and VCAM-1 (APC) on MSCs after 24 h treatment with soluble factors. Gated percent positive population of MSCs compared with the negative population (*black* histogram) are indicated as mean ± SEM on *top right* of overlayed histograms (*red* for CM, *green* for PDGF, *blue* for TGF-β1, and *violet* for PDGF + TGF-β1). Statistical significances are indicated using (*) for $p < 0.05$, (**) for $p < 0.005$, and (***) for $p < 0.0005$. Color images available online at www.liebertpub.com/scd

252

the initial 45,101 probe sets of the Affymetrix Mouse Genome 430 2.0 chip) but fewer probe sets for the combined TGF-β1 and PDGF (8,117 differentially expressed probe sets of FDR 2.13% or 18.0% of the initial 45,101 genes of Affymetrix Mouse Genome 430 2.0 chip). Even fewer probe sets were estimated for PDGF (only 842 differentially expressed probe sets of FDR 1.5% or 1.87% of the initial 45,101 genes of Affymetrix Mouse Genome 430 2.0 chip).

Differentially expressed genes display distinct pathway enrichment in TGF-β1 and PDGF

The number of significantly differentially expressed genes between treatments and controls were 589, 6,751, and 5,292 for the PDGF, TGF-β1, and the combined PDGF and TGF-β1 treatments, respectively (Fig. 5B). The most significantly enriched pathways for each treatment regime are listed in Supplementary Table S1. The most significantly enriched pathway across all treatments was the cell adhesion and ECM remodeling pathway. This is consistent with the observed changes in cell adhesion depicted in Fig. 3. Other significantly enriched pathways among TGF-β1-treated cells were cytoskeletal remodeling and developmental processes related to EMT. Interestingly, these pathways were not enriched after PDGF treatment alone, consistent with a potential role of TGF-β1 in cytoskeletal stiffening. The pathways that were significantly enriched after the combined PDGF and TGF-β1 treatments were a mixture of pathways significantly enriched in one or other of the individual treatments.

TGF-β1 regulates cellular stiffness and morphology via close control of ABPs

The structure and function of cytoskeletal actin is controlled by ABPs (reviewed in [51,71]), which bind to actin filaments and modulate their length, stability, and cytoskeletal attachments. With the high impact of TGF-β1 on cytoskeletal structure, its effects on ABPs were assessed using microarray analysis from curated GO gene sets available from Broad Institute's Molecular Signature Database (MSigDB) (Fig. 5C) [72]. Stabilizing proteins were constitutively upregulated in TGF-β1-treated MSCs, whereas capping and severing proteins were constitutively downregulated (Fig. 5C). Tropomyosin stabilizes actin bundles by protecting them from actin-depolymerization factor/cofilin and interacts with troponin to regulate the interaction of actin and myosin [51]. *Tropomyosin-1* (*Tpm1*) along with *troponin* (*Tnnt2*) were upregulated, whereas its inhibitor *tropomodulin* (*Tmod3*) was downregulated in TGF-β1-treated cells. Bundling and crosslinking proteins regulate cell tension through close association with actin stress fibers. Bundling proteins α-actinin-1 (*Actn1*) and *transgelin* (*Tagln*) were upregulated and other crosslinkers such as *α2 and β2 spectrins* (*Spna2*, *Spnb2*), which play a key role in membrane anchoring of actin, were downregulated. Membrane-anchoring proteins, which tether intracellular domains of actin to membrane proteins, were mostly upregulated with the exception of *ezrin* (*Ezr*) and aforementioned *spectrins*. *Ezr* belongs to ERM family of anchoring proteins with other members being *moesin* (*Msn*) and *radixin* (*Rdx*). *Msn*, which directly regulates cortical rigidity in dividing cells, was upregulated in TGF-β1-treated cells; however, change in *Rdx* expression was not significant. These reg-

ulation patterns of ERM proteins are in agreement with previous studies with TGF-β1-treated epithelial cells [73].

Discussion

MSCs are highly proliferative adult stem cells that are involved in wound healing and tissue regeneration [74]. They have been shown to change their mechanical properties both during differentiation [55] as well as recruitment to sites of inflammation, such as wound sites and tumor tissue [74]. Though soluble factors are critical for both of these processes [75,76], little is known about the effects of individual growth factors on the intracellular mechanical properties of MSCs. In this study, we investigated changes in mechanical properties, including intracellular rheology, cytoskeletal organization, and adhesivity, as well as molecular pathways differentially regulated by 24-h treatment with PDGF-BB (PDGF) and/or TGF-β1.

The cytoskeleton that underlies cell rheological properties is a network of highly heterogeneous and dynamic filamentous proteins that not only provide the cell with structural support but also actively rearrange to permit motility. Alterations in morphology and cytoskeleton have been correlated with changes in the intracellular mechanical properties [19]. Particle-tracking methods probe the local viscoelastic nature of the cell, which is determined from the transport rates of particles embedded in cytoplasm. Particle tracking has been used in vitro to characterize the mechanical properties of networks of reconstituted cytoskeletal proteins [45,77] and in vivo to probe the dynamic mechanical properties of filamentous proteins in the cell cytoskeleton [44]. Kole et al. previously found that Swiss 3T3 fibroblasts that migrate at the edge of a scratch wound assay undergo heterogeneous stiffening response, characterized by increased rigidity of cortical actin, to PDGF treatment [20].

MPTM was used in this study to determine the effects of TGF-β1 and PDGF on the microscopic mechanical properties of MSCs (Fig. 1). MSCs underwent a homogenous stiffening response to TGF-β1 treatment with the cytoplasm transforming into an elastic solid. This homogeneous stiffening response was also seen in PDGF- and TGF-β1-treated cells; however, the elasticity of the cytoplasm was increased further 10-fold ($P < 0.05$) with addition of PDGF. These marked shifts in viscoelastic properties of cells may be due to enhanced crosslinking among actin filaments, as similar mechanical strengthening of in vitro actin solutions is demonstrated from the formation of both orthogonal networks and ordered bundles, mediated by F-actin crosslinking/bundling proteins. In vitro, α-actinin increased actin solution elasticity by 15-fold, at a molar ratio of 1:50 (0.03 μM α-actinin in 15 μM actin) [78]. Further studies with other crosslinking (Filamin) and bundling proteins (Fascin) individually or in combination with α-actinin increased the formation of entangled and crosslinked structures of bundled fibers, resulting in stiffer actin gel mechanics [77,79]. The difference in elasticity of combination of PDGF- and TGF-β1-treated cells compared with TGF-β1 alone may be due to a more balanced role between crosslinkers and bundlers, which gives rise to superior ordered architecture with higher stiffness. This surprising result highlights the importance of studying the effects of soluble factors on the mechanical
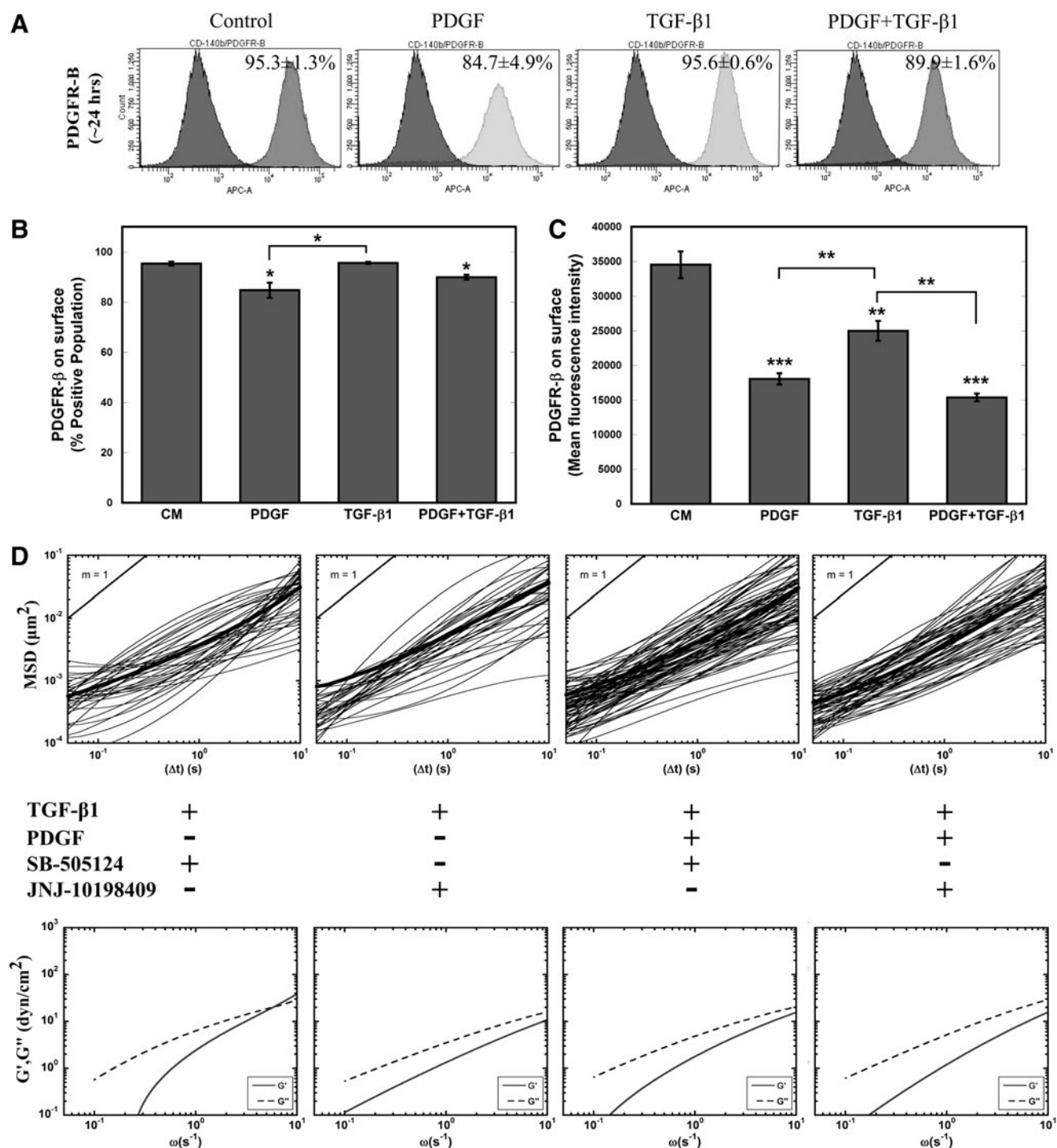
FIG. 4. Role of PDGFR-β in TGF-β1 signaling. **(A)** Flow cytometric analysis of surface PDGFR-β expression on MSCs in response to soluble factor treatment at 24 h. **(B, C)** Percent positive population and MFI of treated cells were calculated from FACS-DIVA. PDGF and combination of PDGF and TGF-β1 resulted in reduced available surface receptors after 24 h; TGF-β1 treatment also reduced available PDGFR-β. Results are reported as average ± SEM ($n=3$). **(D)** Effect of small-molecule chemical inhibitors SB-505124 (blocks TGF-βRI-mediated signaling) and JNJ-10198409 (inhibits PDGFR-β-mediated signaling) on the viscoelastic properties of soluble-factor-treated MSCs were evaluated after 24 h. The average mean squared displacements of 100-nm particles embedded in the cytoplasm of cells and frequency-dependent elastic (G') and viscous (G'') moduli of inhibitor-treated MSCs were similar to the control cells (Fig. 2A, B). Statistical significances are indicated as (*) for $p < 0.05$, (**) for $p < 0.005$, and (***) for $p < 0.0005$.
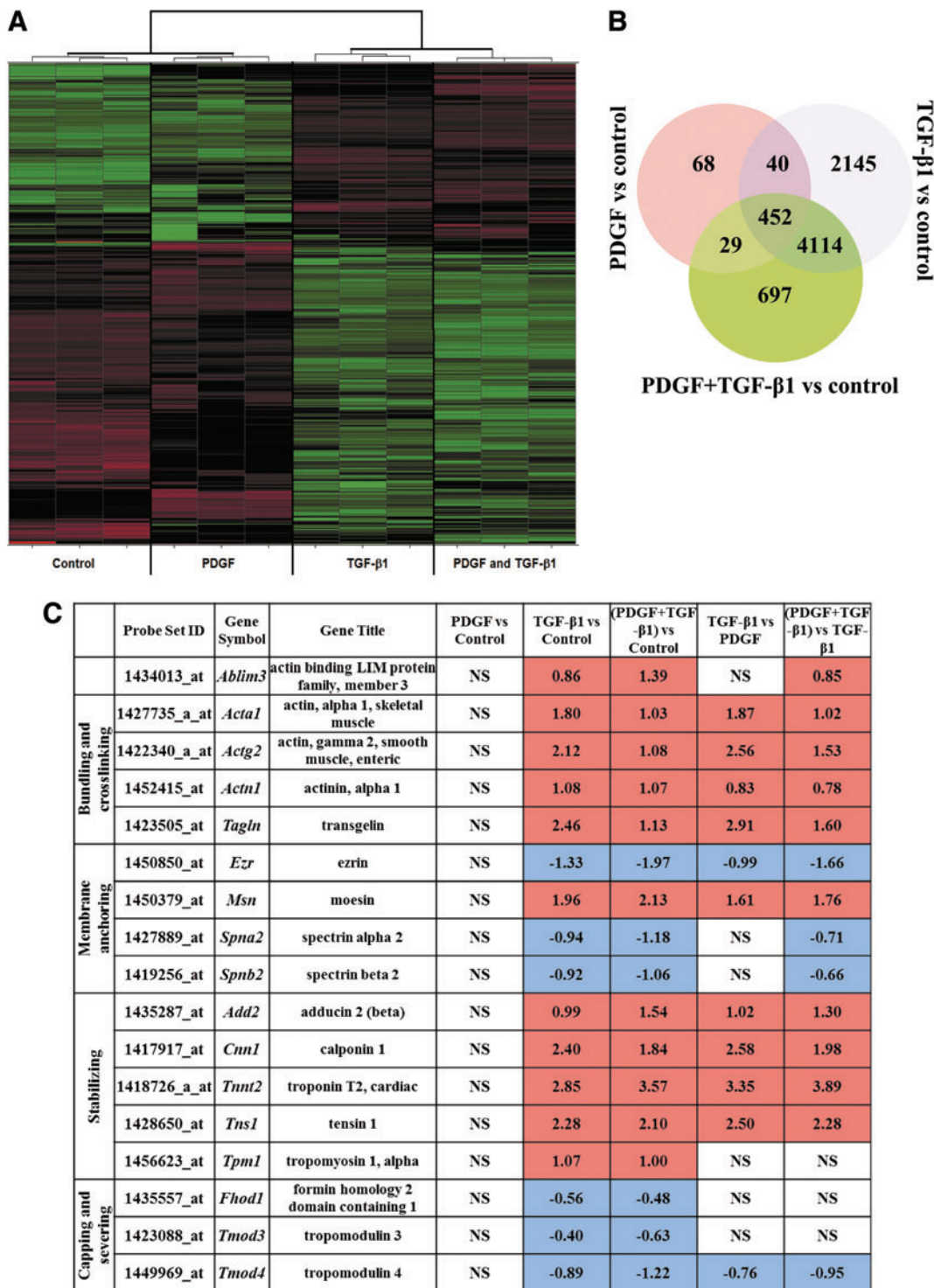
FIG. 5. Effects on MSC genomic profiles of treatment with PDGF, TGF-β1, and combination of PDGF and TGF-β1. **(A)** Heatmap indicates significant changes (false discovery rate *P*-value ≤ 0.05) in gene expression (*black*, no change; *red*, increase; *green*, decrease) due to serum-free, PDGF, TGF-β1, and combination of PDGF and TGF-β1 (*n* = 3). **(B)** Venn diagram depicts the number of genes regulated in a soluble factor treatment–specific and –nonspecific manner within each segment (*n* = 3). **(C)** Regulation of actin-binding proteins (ABPs) in response to soluble factor treatment (*n* = 3). Color images available online at www.liebertpub.com/scd

properties of MSCs. Differences in the viscoelastic behavior of cells have been associated with differentiation potential [80], malignant transformation, and disease [81]. For instance, activation of latent TGF-β1 in soft tissues, such as the kidney, has been deemed critical for tissue fibrosis [82],

which may be due to stiffening of both cells and their remodeled environments.

We further investigated more macroscopic cytoskeletal changes in response to TGF-β1 and PDGF by evaluating the CSF and actin stress fiber density. Treatment with TGF-β1,
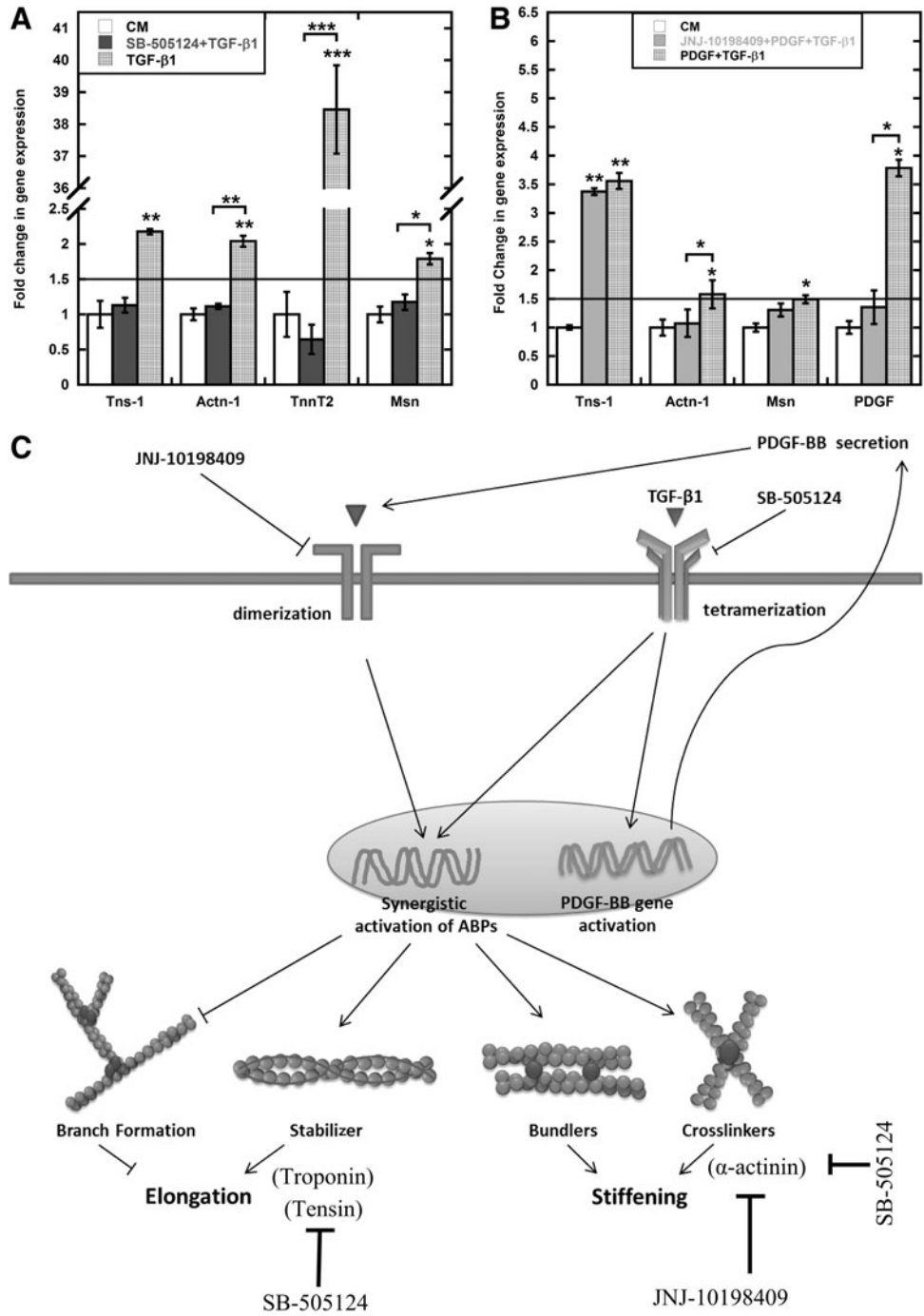
FIG. 6. PDGF signaling influences TGF-β1-mediated mechanical stiffening. **(A)** SB-505124 blocked the upregulation of TGF-β1-mediated expression of ABPs *tensin-1* (*Tns-1*), *alpha-actinin-1* (*Actn1*), *troponin T2* (*Tnnt2*), and *moesin* (*Msn*) compared with control after 24 h. **(B)** JNJ-10198409 selectively blocked *Actn1* and p*dgfb* gene activation in PDGF- and TGF-β1-treated cells compared with control. Gene expression was normalized using 18sRNA as internal control. Results are reported as average±SEM (*n*=3). **(C)** A simplified diagram correlating mechanical response of MSCs to treatment with TGF-β1 by molecular regulation of ABPs, for example, actin stabilization and crosslinking. After 24 h exposure to TGF-β1, alterations in morphology and stiffness can be explained by differential gene expression in ABPs. Statistical significances are shown as (*) for $p<0.05$, (**) for $p<0.005$, and (***) for $p<0.0005$.

but not PDGF, resulted in increased stress fiber density and cell elongation. Surprisingly, the effect of TGF-β1 was enhanced by the addition of PDGF, indicating that crosstalk in signaling pathways is important in mediating this response (Fig. 2). Interestingly, TGF-β1-treated cells were aligned in parallel but introduction of PDGF with TGF-β1 increased the randomness in their orientation. The parallel alignment of TGF-β1-treated cells may be associated with increased production of fibrillar collagen [83,84]. Mannose-6-phosphate [85] and other TGF-β inhibitors [86,87] are used to prevent hypertrophic scars, which are often associated with increased collage I expression and parallel alignment of ECM proteins.

TGF-β1 is also known for its role in directing MSC differentiation into bone, cartilage, and muscle [88] and for regulating the expression of other growth factors, including PDGF [89], important in stem cell growth, maintenance, and differentiation [90]. Although PDGF and TGF-β1 affect many cellular processes over longer time periods, the molecular and mechanical response to these factors was measured after a 24-h exposure, which minimizes the effects of these processes on cellular mechanics. Over the 24-h time period used in our studies, PDGF and TGF-β1 did not affect MSC differentiation, as determined by genetic and histological screening; however, 24-h incubation with TGF-β1 resulted in

increased expression of cytokine and growth factor genes (Supplementary Table S2). Though these factors may contribute to intracellular mechanical changes, in physiologically relevant environments they would be impossible to decouple, so for this study we limited in-depth microarray analysis to a subset of the microarray data that involve genes that code for cytoskeletal proteins.

Direct signal propagation through TGF-β pathways, both SMAD dependent and independent, combined with intracellular tension resulted in very high numbers of regulated genes as determined by microarray experiments. Previous studies have explored molecular mechanism behind TGF-β1-dependent cytoskeletal remodeling and found important roles of small Rho-GTPases (RhoA, CDC42, and Rac1) [91–93]. To understand cytoskeletal reorganization and mechanical stiffening response, we focused on genes that encode for ABPs that directly control actin remodeling [51,71]. The filamentous actin cytoskeletal network is regulated by several classes of ABPs: crosslinkers and bundlers, which construct higher-order network structure; stabilizers that sustain unidirectional growth and protection from severing; nucleation and branch-forming proteins, which initiate filament formation; and monomer binders and capping and severing proteins control the polymerization and depolymerization of actin filaments. Cells treated with TGF-β1 and combination of PDGF and TGF-β1 upregulated gene expression of bundling, crosslinking, and stabilizing proteins. Other groups of proteins associated with branch formation, capping, and severing were generally downregulated, facilitating unidirectional growth of actin filaments and stress fibers.

Crosslinking and bundling proteins can affect both the overall network architecture and the ability to dynamically reorganize these networks. The ABP α-actinin acts as a crosslinker and bundler in reconstituted actin solutions [94] and organizes F-actin filaments in orthogonal or parallel structures in cells, contributing to both stress fiber formation and cellular stiffness [79]. Other proteins like fascin and transgelin interact more selectively with F-actin, which is important for generating more structured actin networks like parallel bundles found in filopodia and stress fiber formation [95–97]. Increasing the thickness of these parallel bundles or reducing the degrees of freedom for polymeric actin movement through orthogonal crosslinking may contribute to high cell stiffness.

Cell–matrix interactions are directly related to intracellular mechanical properties, since the acto-myosin network is connected to the external environment through focal adhesion complexes with the ECM [98]. TGF-β1 treatment induced significant increase in both cell adhesion ($P < 0.0005$ for plastic) and integrin expression ($P < 0.0005$). Addition of PDGF did not enhance the adhesion effect of TGF-β1, indicating that crosstalk between these signaling pathways is likely not important in ECM remodeling and adhesion. MSC treatment with TGF-β1 also resulted in enhanced expression of matrix proteins, like collagen (Col), fibronectin (Fbn), and tenascin (Tnc), and matrix metalloproteinases (Mmp) (Supplementary Table S2) that are important in remodeling the ECM of the wound bed and tumor microenvironment. Intracellular mechanical forces on the local environment may induce further remodeling of the ECM through physical interactions. Taken together, these results suggest that TGF-β1 has a profound role in controlling the individual cell and overall tissue mechanical behavior in tumors and wound sites.

Due to the complexities of intracellular control of actin mechanics that originates from protein interactions and post-translation modifications, it is difficult to isolate the mechanical response to a particular protein or protein complex. Instead we focused on the roles of the principal signaling pathways affected by TGF-β1 and PDGF. The initial studies suggested that PDGF can augment effect of TGF-β1. Multiple studies have provided evidence of crosstalk between these two pathways [99,100]. We used small-molecule receptor inhibitors to explore the role of PDGF and TGF-β1 signaling in the mechanical response (Fig. 4D). SB-505124 binds to TGF-βRI and inhibits phosphorylation of Smad2/3 to block TGF-β signaling. It has been shown to successfully block recruitment of MSCs to injured arteries [101] and block ALK5-mediated chondrogenesis of MSCs [64]. JNJ-10198409 is PDGFR-β tyrosine kinase inhibitor and it has been primarily examined to inhibit proliferation of different cell types [66,102]. Both inhibitors have been tested independently to curb tumor growth, although through different mechanisms [66,103]. SB-505124 expectedly inhibited elongation and stiffening response; however, more interestingly, PDGFR-β inhibitor JNJ-10198409 blocked these responses as well for both TGF-β1 alone and in combination with PDGF. We further investigated role of these inhibitors on relevant gene activation, that is, ABPs, such as tensin-1 (Tns1), α-actinin-1 (Actn1), troponin t2 (Tnnt2), and moesin (Msn), using PCR and gel electrophoresis. After initial screening, we focused on four genes for each inhibitor based on differential response. SB-505124 completely blocked the TGF-β1-mediated upregulation of all four genes (Fig. 6A). Since PDGF individually does not regulate ABPs, we used JNJ-10198409 to examine the role of PDGF signaling in combined soluble-factor-treated cells. Expectedly, JNJ-10198409 abrogated Pdgfb gene activation (Fig. 6B). More interestingly, it selectively only blocked Actn1 activation. Combined with the previous results of complete inhibition of TGF-β1-mediated cell stiffening with JNJ-10198409, this data suggests that Actn1 is one of the key regulators of cell stiffening. However, a more detailed screening of ABPs with JNJ-10198409 is required to explore all the key elements of stiffening response. These studies provided evidence of integral role of PDGFR-β-mediated signaling for individual TGF-β1 treatment. Further, two different time scales, including short (∼1 h) (Supplementary Fig. S1C, E) and long (∼24 h), were used to determine possible interaction between TGF-β1 treatment and PDGFR-β expression. At short time scale, available surface PDGFR-β expression was downregulated for PDGF-treated cells individually and in combination with TGF-β1 compared with control [both by PPC and MFI (Supplementary Fig. S1E)]. Similar trends were found to be true at longer time scale for PDGF and combination of PDGF and TGF-β1 (Fig. 4A–C). For TGF-β1-treated cells, surface expression of PDGFR-β was comparable to that of control cells at shorter time scale. However, surface expression of PDGFR-β on TGF-β1-treated cells was significantly ($P < 0.005$) lower compared with control cells after 24 h (Fig. 4B). Analysis of microarray data exhibits 0.5-fold ($P < 0.05$) increase in PDGFB expression for TGF-β1-treated cells compared with control. This result was also confirmed using PCR (Supplementary Fig. S2).

Data presented here strongly indicate crosstalk between PDGF and TGF-β1 signaling pathways in regulating certain aspects of the mechanical and chemical response of MSCs.

Upregulation of *Pdgfb* and *Pdgfrb* in TGF-β1-treated cells might be due to the autocrine induction of PDGF signaling (Fig. 6C). Other studies have suggested establishment of the autocrine PDGF-loop in TGF-β1-treated cells although in different cell types [104,105]. This study suggests that this PDGF loop may be integral for TGF-β1-mediated mechanical response. And for combination treatment, addition of recombinant PDGF protein amplifies the response from PDGF loop that later interacts with intracellular TGF-β1 signaling to modulate the rheological and cytoskeletal response.

Conclusions

TGF-β1 is essential for normal tissue remodeling and wound healing and plays an important role in the development of epithelial malignancies [106,107]. The TGF-β1 signaling pathway is manipulated in numerous therapeutic applications from regenerative medicine to cancer. This study indicates at the cellular level that TGF-β1 can induce cytoskeletal remodeling to change cell rheology and shape, and increase integrin-dependent adhesion strength to modify cell behavior. This study shows that PDGF may be a viable target in manipulating certain aspects of this signaling pathway.

In recent years biophysical cues are extensively investigated in regulating cellular function [14,16,98]. Matrix rigidity in concert with soluble factors has been shown to affect stem cell migration, proliferation, and differentiation. In future studies, matrix substrate compliance will be added as a variable to further our understanding of MSC response to soluble factors.

Acknowledgments

Author Disclosure Statement

No competing financial interests exist.

References

1. Caplan AI. (2007). Adult mesenchymal stem cells for tissue engineering versus regenerative medicine. J Cell Physiol 213:341–347.

2. Caplan AI and SP Bruder. (2001). Mesenchymal stem cells: building blocks for molecular medicine in the 21st century. Trends Mol Med 7:259–264.

3. da Silva Meirelles L, PC Chagastelles and NB Nardi. (2006). Mesenchymal stem cells reside in virtually all post-natal organs and tissues. J Cell Sci 119:2204–2213.

4. Pittenger MF, AM Mackay, SC Beck, RK Jaiswal, R Douglas, JD Mosca, MA Moorman, DW Simonetti, S Craig and DR Marshak. (1999). Multilineage potential of adult human mesenchymal stem cells. Science 284:143–147.

5. Phinney DG and DJ Prockop. (2007). Concise review: mesenchymal stem/multipotent stromal cells: the state of transdifferentiation and modes of tissue repair—current views. Stem Cells 25:2896–2902.

6. Chamberlain G, J Fox, B Ashton and J Middleton. (2007). Concise review: mesenchymal stem cells: their phenotype, differentiation capacity, immunological features, and potential for homing. Stem Cells 25:2739–2749.

7. Parekkadan B and JM Milwid. (2010). Mesenchymal stem cells as therapeutics. Annu Rev Biomed Eng 12:87–117.

8. Williams AR and JM Hare. (2011). Mesenchymal stem cells biology, pathophysiology, translational findings, and therapeutic implications for cardiac disease. Circ Res 109:923–940.

9. Lee RH, MJ Seo, RL Reger, JL Spees, AA Pulin, SD Olson and DJ Prockop. (2006). Multipotent stromal cells from human marrow home to and promote repair of pancreatic islets and renal glomeruli in diabetic NOD/scid mice. Proc Natl Acad Sci U S A 103:17438–17443.

10. Németh K, A Leelahavanichkul, PS Yuen, B Mayer, A Parmelee, K Doi, PG Robey, K Leelahavanichkul, BH Koller and JM Brown. (2008). Bone marrow stromal cells attenuate sepsis via prostaglandin E2-dependent reprogramming of host macrophages to increase their interleukin-10 production. Nat Med 15:42–49.

11. Gupta N, X Su, B Popov, JW Lee, V Serikov and MA Matthay. (2007). Intrapulmonary delivery of bone marrow-derived mesenchymal stem cells improves survival and attenuates endotoxin-induced acute lung injury in mice. J Immunol 179:1855–1863.

12. Wu Y, J Wang, PG Scott and EE Tredget. (2007). Bone marrow-derived stem cells in wound healing: a review. Wound Repair Regen 15:S18–S26.

13. Maxson S, EA Lopez, D Yoo, A Danilkovitch-Miagkova and MA LeRoux. (2012). Concise review: role of mesenchymal stem cells in wound repair. Stem Cells Transl Med 1:142–149.

14. Discher DE, DJ Mooney and PW Zandstra. (2009). Growth factors, matrices, and forces combine and control stem cells. Science 324:1673–1677.

15. McBeath R, DM Pirone, CM Nelson, K Bhadriraju and CS Chen. (2004). Cell shape, cytoskeletal tension, and RhoA regulate stem cell lineage commitment. Dev Cell 6:483–495.

16. Engler A, S Sen, H Sweeney and D Discher. (2006). Matrix elasticity directs stem cell lineage specification. Cell 126:677–689.

17. Wang L, Y Li, X Chen, J Chen, S Gautam, Y Xu and M Chopp. (2002). MCP-1, MIP-1, IL-8 and ischemic cerebral tissue enhance human bone marrow stromal cell migration in interface culture. Hematology 7:113–117.

18. Ji JF, BP He, ST Dheen and SSW Tay. (2004). Interactions of chemokines and chemokine receptors mediate the migration of mesenchymal stem cells to the impaired site in the brain after hypoglossal nerve injury. Stem Cells 22:415–427.

19. McGrail DJ, D Ghosh, ND Quach and MR Dawson. (2012). Differential mechanical response of mesenchymal stem cells and fibroblasts to tumor-secreted soluble factors. PloS One 7:e33248.

20. Kole TP, Y Tseng, I Jiang, JL Katz and D Wirtz. (2005). Intracellular mechanics of migrating fibroblasts. Mol Biol Cell 16:328–338.

21. McGrail DJ, KM McAndrews and MR Dawson. (2012). Biomechanical analysis predicts decreased human mesenchymal stem cell function before molecular differences. Exp Cell Res 319:684–696.

22. Klopp AH, EL Spaeth, JL Dembinski, WA Woodward, A Munshi, RE Meyn, JD Cox, M Andreeff and FC Marini. (2007). Tumor irradiation increases the recruitment of circulating mesenchymal stem cells into the tumor microenvironment. Cancer Res 67:11687–11695.

23. Birnbaum T, J Roider, C Schankin, C Padovan, C Schichor, R Goldbrunner and A Straube. (2007). Malignant gliomas

actively recruit bone marrow stromal cells by secreting angiogenic cytokines. J Neurooncol 83:241–247.

24. Dittmar T and F Entschladen. (2013). Migratory properties of mesenchymal stem cells. In: *Mesenchymal Stem Cells—Basics and Clinical Application I.* Weyand B, M Dominici, R Hass, R Jacobs and C Kasper, eds. Springer Berlin Heidelberg, pp 117–136.

25. Derynck R and K Miyazono. (2008). *The TGF-[beta] family.* Cold Spring Harbor Laboratory Press, Cold Spring Harbor, New York.

26. Massagué J. (1998). TGF-β signal transduction. Annu Rev Biochem 67:753–791.

27. Derynck R and YE Zhang. (2003). Smad-dependent and Smad-independent pathways in TGF-β family signalling. Nature 425:577–584.

28. Crowe MJ, T Doetschman and DG Greenhalgh. (2000). Delayed wound healing in immunodeficient TGF-beta 1 knockout mice. J Invest Dermatol 115:3–11.

29. Hanahan D and RA Weinberg. (2000). The hallmarks of cancer. Cell 100:57–70.

30. Moustakas A, K Pardali, A Gaal and CH Heldin. (2002). Mechanisms of TGF-beta signaling in regulation of cell growth and differentiation. Immunol Lett 82:85–91.

31. Margadant C and A Sonnenberg. (2010). Integrin-TGF-β crosstalk in fibrosis, cancer and wound healing. EMBO Rep 11:97–105.

32. Epstein FH, GC Blobe, WP Schiemann and HF Lodish. (2000). Role of transforming growth factor β in human disease. N Engl J Med 342:1350–1358.

33. Leight JL, MA Wozniak, S Chen, ML Lynch and CS Chen. (2012). Matrix rigidity regulates a switch between TGF-beta1-induced apoptosis and epithelial-mesenchymal transition. Mol Biol Cell 23:781–791.

34. Orimo A and RA Weinberg. (2006). Stromal fibroblasts in cancer: a novel tumor-promoting cell type. Cell Cycle 5:1597–1601.

35. Chen W and SM Wahl. (1999). Manipulation of TGF-beta to control autoimmune and chronic inflammatory diseases. Microbes Infect 1:1367–1380.

36. Yingling JM, KL Blanchard and JS Sawyer. (2004). Development of TGF-β signalling inhibitors for cancer therapy. Nat Rev Drug Discov 3:1011–1022.

37. Ponte AL, E Marais, N Gallay, A Langonne, B Delorme, O Herault, P Charbord and J Domenech. (2007). The *in vitro* migration capacity of human bone marrow mesenchymal stem cells: comparison of chemokine and growth factor chemotactic activities. Stem Cells 25:1737–1745.

38. Fiedler J, G Röderer, KP Günther and RE Brenner. (2002). BMP-2, BMP-4, and PDGF-bb stimulate chemotactic migration of primary human mesenchymal progenitor cells. J Cell Biochem 87:305–312.

39. Andrae J, R Gallini and C Betsholtz. (2008). Role of platelet-derived growth factors in physiology and medicine. Genes Dev 22:1276–1312.

40. Betsholtz C, L Karlsson and P Lindahl. (2001). Developmental roles of platelet-derived growth factors. BioEssays 23:494–507.

41. Betsholtz C. (2004). Insight into the physiological functions of PDGF through genetic studies in mice. Cytokine Growth Factor Rev 15:215–228.

42. Ball SG, CA Shuttleworth and CM Kielty. (2007). Platelet-derived growth factor receptor-[alpha] is a key determinant of smooth muscle [alpha]-actin filaments in bone marrow-derived mesenchymal stem cells. Int J Biochem Cell Biol 39:379–391.

43. Jechlinger M, A Sommer, R Moriggl, P Seither, N Kraut, P Capodiecci, M Donovan, C Cordon-Cardo, H Beug and S Grünert. (2006). Autocrine PDGFR signaling promotes mammary cancer metastasis. J Clin Invest 116:1561–1570.

44. Kole TP, Y Tseng and D Wirtz. (2004). Intracellular microrheology as a tool for the measurement of the local mechanical properties of live cells. Methods Cell Biol 78:45–64.

45. Tseng Y, E Fedorov, JM McCaffery, SC Almo and D Wirtz. (2001). Micromechanics and ultrastructure of actin filament networks crosslinked by human fascin: a comparison with alpha-actinin. J Mol Biol 310:351–366.

46. Engler AJ, MA Griffin, S Sen, CG Bonnemann, HL Sweeney and DE Discher. (2004). Myotubes differentiate optimally on substrates with tissue-like stiffness: pathological implications for soft or stiff microenvironments. J Cell Biol 166:877–887.

47. Kole TP, Y Tseng, L Huang, JL Katz and D Wirtz. (2004). Rho kinase regulates the intracellular micromechanical response of adherent cells to rho activation. Mol Biol Cell 15:3475–3484.

48. Wirtz D. (2009). Particle-tracking microrheology of living cells: principles and applications. Annu Rev Biophys 38:301–326.

49. Treiser MD, EH Yang, S Gordonov, DM Cohen, IP Androulakis, J Kohn, CS Chen and PV Moghe. (2010). Cytoskeleton-based forecasting of stem cell lineage fates. Proc Natl Acad Sci U S A 107:610–615.

50. Kilian KA, B Bugarija, BT Lahn and M Mrksich. (2010). Geometric cues for directing the differentiation of mesenchymal stem cells. Proc Natl Acad Sci U S A 107:4872–4877.

51. Winder SJ and KR Ayscough. (2005). Actin-binding proteins. J Cell Sci 118:651–654.

52. Sun Y, CS Chen and J Fu. (2012). Forcing stem cells to behave: a biophysical perspective of the cellular microenvironment. Annu Rev Biophys 41:519–542.

53. Pullarkat PA, PA Fernández and A Ott. (2007). Rheological properties of the eukaryotic cell cytoskeleton. Phys Rep 449:29–53.

54. Byfield FJ, RK Reen, T-P Shentu, I Levitan and KJ Gooch. (2009). Endothelial actin and cell stiffness is modulated by substrate stiffness in 2D and 3D. J Biomech 42:1114–1119.

55. Darling EM, M Topel, S Zauscher, TP Vail and F Guilak. (2008). Viscoelastic properties of human mesenchymally-derived stem cells and primary osteoblasts, chondrocytes, and adipocytes. J Biomech 41:454–464.

56. Pang C, Z Gao, J Yin, J Zhang, W Jia and J Ye. (2008). Macrophage infiltration into adipose tissue may promote angiogenesis for adipose tissue remodeling in obesity. Am J Physiol Endocrinol Metab 295:E313–E322.

57. Leitzel K, W Bryce, J Tomita, G Manderino, I Tribby, A Thomason, M Billingsley, E Podczaski, H Harvey and M Bartholomew. (1991). Elevated plasma platelet-derived growth factor B-chain levels in cancer patients. Cancer Res 51:4149–4154.

58. Hudkins KL, DG Gilbertson, M Carling, S Taneda, SD Hughes, MS Holdren, TE Palmer, S Topouzis, AC Haran and AL Feldhaus. (2004). Exogenous PDGF-D is a potent mesangial cell mitogen and causes a severe mesangial proliferative glomerulopathy. J Am Soc Nephrol 15:286–298.

59. Meyer A, W Wang, J Qu, L Croft, JL Degen, BS Coller and J Ahamed. (2012). Platelet TGF-β1 contributions to plasma TGF-β1, cardiac fibrosis, and systolic dysfunction in a mouse model of pressure overload. Blood 119:1064–1074.

60. Wakefield LM, JJ Letterio, T Chen, D Danielpour, RS Allison, LH Pai, AM Denicoff, MH Noone, KH Cowan and JA O'Shaughnessy. (1995). Transforming growth factor-beta1 circulates in normal human plasma and is unchanged in advanced metastatic breast cancer. Clin Cancer Res 1:129–136.

61. Kortesidis A, A Zannettino, S Isenmann, S Shi, T Lapidot and S Gronthos. (2005). Stromal-derived factor-1 promotes the growth, survival, and development of human bone marrow stromal stem cells. Blood 105:3793–3801.

62. Cassiede P, JE Dennis, F Ma and AI Caplan. (1996). Osteochondrogenic potential of marrow mesenchymal progenitor cells exposed to TGF-β1 or PDGF-BB as assayed *in vivo* and *in vitro*. J Bone Miner Res 11:1264–1273.

63. Tang Y, X Wu, W Lei, L Pang, C Wan, Z Shi, L Zhao, TR Nagy, X Peng and J Hu. (2009). TGF-β1-induced migration of bone mesenchymal stem cells couples bone resorption with formation. Nat Med 15:757–765.

64. Hellingman CA, ENB Davidson, W Koevoet, EL Vitters, WB van den Berg, GJ van Osch and PM van der Kraan. (2011). Smad signaling determines chondrogenic differentiation of bone-marrow-derived mesenchymal stem cells: inhibition of Smad1/5/8P prevents terminal differentiation and calcification. Tissue Eng Part A 17:1157–1167.

65. Fujitani M, N Grinshtein, KM Smith and DR Kaplan. (2012). Potent and selective cytotoxic and cytostatic activity of JNJ-10198409 against neuroblastoma cells. Chiba Med J 88:27–34.

66. D'Andrea MR, JM Mei, RW Tuman, RA Galemmo and DL Johnson. (2005). Validation of *in vivo* pharmacodynamic activity of a novel PDGF receptor tyrosine kinase inhibitor using immunohistochemistry and quantitative image analysis. Mol Cancer Therapeut 4:1198–1204.

67. Tee S-Y, J Fu, CS Chen and PA Janmey. (2011). Cell shape and substrate rigidity both regulate cell stiffness. Biophys J 100:L25–L27.

68. DaCosta Byfield S, C Major, NJ Laping and AB Roberts. (2004). SB-505124 is a selective inhibitor of transforming growth factor-β type I receptors ALK4, ALK5, and ALK7. Mol Pharmacol 65:744–752.

69. Ho CY, DW Ludovici, US Maharoof, J Mei, JL Sechler, RW Tuman, ED Strobel, L Andraka, H-K Yen and G Leo. (2005). (6, 7-Dimethoxy-2, 4-dihydroindeno [1, 2-c] pyrazol-3-yl) phenylamines: platelet-derived growth factor receptor tyrosine kinase inhibitors with broad antiproliferative activity against tumor cells. J Med Chem 48:8163–8173.

70. Tusher VG, R Tibshirani and G Chu. (2001). Significance analysis of microarrays applied to the ionizing radiation response. Proc Natl Acad Sci U S A 98:5116–5121.

71. Uribe R and D Jay. (2009). A review of actin binding proteins: new perspectives. Mol Biol Rep 36:121–125.

72. Subramanian A, P Tamayo, VK Mootha, S Mukherjee, BL Ebert, MA Gillette, A Paulovich, SL Pomeroy, TR Golub, ES Lander and JP Mesirov. (2005). Gene set enrichment analysis: a knowledge-based approach for interpreting genome-wide expression profiles. Proc Natl Acad Sci U S A 102:15545–15550.

73. Haynes J, J Srivastava, N Madson, T Wittmann and DL Barber. (2011). Dynamic actin remodeling during epithelial–mesenchymal transition depends on increased moesin expression. Mol Biol Cell 22:4750–4764.

74. Djouad F, P Plence, C Bony, P Tropel, F Apparailly, J Sany, D Noel and C Jorgensen. (2003). Immunosuppressive effect of mesenchymal stem cells favors tumor growth in allogeneic animals. Blood 102:3837–3844.

75. Barrientos S, O Stojadinovic, MS Golinko, H Brem and M Tomic-Canic. (2008). Growth factors and cytokines in wound healing. Wound Repair Regen 16:585–601.

76. Hanahan D and RA Weinberg. (2011). Hallmarks of cancer: the next generation. Cell 144:646–674.

77. Esue O, Y Tseng and D Wirtz. (2009). α-Actinin and filamin cooperatively enhance the stiffness of actin filament networks. PLoS One 4:e4411.

78. Xu J, D Wirtz and TD Pollard. (1998). Dynamic cross-linking by α-actinin determines the mechanical properties of actin filament networks. J Biol Chem 273:9570–9576.

79. Tseng Y, TP Kole, JS Lee, E Fedorov, SC Almo, BW Schafer and D Wirtz. (2005). How actin crosslinking and bundling proteins cooperate to generate an enhanced cell mechanical response. Biochem Biophys Res Commun 334:183–192.

80. González-Cruz RD, VC Fonseca and EM Darling. (2012). Cellular mechanical properties reflect the differentiation potential of adipose-derived mesenchymal stem cells. Proc Natl Acad Sci U S A 109:E1523–E1529.

81. Guck J, S Schinkinger, B Lincoln, F Wottawah, S Ebert, M Romeyke, D Lenz, HM Erickson, R Ananthakrishnan and D Mitchell. (2005). Optical deformability as an inherent cell marker for testing malignant transformation and metastatic competence. Biophys J 88:3689–3698.

82. Pohlers D, J Brenmoehl, I Löffler, CK Müller, C Leipner, S Schultze-Mosgau, A Stallmach, RW Kinne and G Wolf. (2009). TGF-β and fibrosis in different organs—molecular pathway imprints. Biochim Biophys Acta 1792:746–756.

83. Warstat K, D Meckbach, M Weis-Klemm, A Hack, G Klein, P de Zwart and WK Aicher. (2010). TGF-beta enhances the integrin alpha2beta1-mediated attachment of mesenchymal stem cells to type I collagen. Stem Cells Dev 19:645–656.

84. D'Angelo M, JM Chen, K Ugen and RM Greene. (1994). TGF beta 1 regulation of collagen metabolism by embryonic palate mesenchymal cells. J Exp Zool 270:189–201.

85. Xia C, XY Yang, Y Wang and S Tian. (2011). Inhibition effect of mannose-6-phosphate on expression of transforming growth factor Beta receptor in flexor tendon cells. Orthopedics 34:21.

86. Zhang Z, TM Garron, XJ Li, Y Liu, X Zhang, YY Li and WS Xu. (2009). Recombinant human decorin inhibits TGF-beta1-induced contraction of collagen lattice by hypertrophic scar fibroblasts. Burns 35:527–537.

87. Lu L, AS Saulis, WR Liu, NK Roy, JD Chao, S Ledbetter and TA Mustoe. (2005). The temporal effects of anti-TGF-beta1, 2, and 3 monoclonal antibody on wound healing and hypertrophic scar formation. J Am Coll Surg 201:391–397.

88. Park JS, JS Chu, AD Tsou, R Diop, Z Tang, A Wang and S Li. (2011). The effect of matrix stiffness on the differentiation of mesenchymal stem cells in response to TGF-beta. Biomaterials 32:3921–3930.

89. Zhao F, YF Zhang, YG Liu, JJ Zhou, ZK Li, CG Wu and HW Qi. (2008). Therapeutic effects of bone marrow-derived mesenchymal stem cells engraftment on bleomycin-induced lung injury in rats. Transplant Proc 40:1700–1705.

90. Ng F, S Boucher, S Koh, KS Sastry, L Chase, U Lakshmipathy, C Choong, Z Yang, MC Vemuri, MS Rao and V Tanavde. (2008). PDGF, TGF-beta, and FGF signaling is important for differentiation and growth of mesenchymal stem cells (MSCs): transcriptional profiling can identify markers and signaling pathways important in differentiation of MSCs into adipogenic, chondrogenic, and osteogenic lineages. Blood 112:295–307.

91. Edlund S, M Landstrom, C-H Heldin and P Aspenstrom. (2002). Transforming Growth factor-beta-induced mobilization of actin cytoskeleton requires signaling by Small GTPases Cdc42 and RhoA. Mol Biol Cell 13:902–914.

92. Vardouli L, E Vasilaki, E Papadimitriou, D Kardassis and C Stournaras. (2008). A novel mechanism of TGFβ-induced actin reorganization mediated by Smad proteins and Rho GTPases. FEBS J 275:4074–4087.

93. Arber S, FA Barbayannis, H Hanser, C Schneider, CA Stanyon, O Bernard and P Caroni. (1998). Regulation of actin dynamics through phosphorylation of cofilin by LIM-kinase. Nature 393:805–809.

94. Wachsstock DH, W Schwartz and TD Pollard. (1993). Affinity of alpha-actinin for actin determines the structure and mechanical properties of actin filament gels. Biophys J 65:205–214.

95. Tojkander S, G Gateva and P Lappalainen. (2012). Actin stress fibers—assembly, dynamics and biological roles. J Cell Sci 125:1855–1864.

96. Goodman A, BL Goode, P Matsudaira and GR Fink. (2003). The *Saccharomyces cerevisiae* calponin/transgelin homolog Scp1 functions with fimbrin to regulate stability and organization of the actin cytoskeleton. Mol Biol Cell 14:2617–2629.

97. Vignjevic D, S-i Kojima, Y Aratyn, O Danciu, T Svitkina and GG Borisy. (2006). Role of fascin in filopodial protrusion. J Cell Biol 174:863–875.

98. Discher DE, P Janmey and Y-l Wang. (2005). Tissue cells feel and respond to the stiffness of their substrate. Science 310:1139–1143.

99. Qi Y-X, J Jiang, X-H Jiang, X-D Wang, S-Y Ji, Y Han, D-K Long, B-R Shen, Z-Q Yan and S Chien. (2011). PDGF-BB and TGF-β1 on cross-talk between endothelial and smooth muscle cells in vascular remodeling induced by low shear stress. Proc Natl Acad Sci U S A 108:1908–1913.

100. Leof EB, JA Proper, AS Goustin, GD Shipley, PE DiCorleto and HL Moses. (1986). Induction of c-sis mRNA and activity similar to platelet-derived growth factor by transforming growth factor beta: a proposed model for indirect mitogenesis involving autocrine activity. Proc Natl Acad Sci U S A 83:2453–2457.

101. Wan M, C Li, G Zhen, K Jiao, W He, X Jia, W Wang, C Shi, Q Xing and YF Chen. (2012). Injury-activated transforming growth factor β controls mobilization of mesenchymal stem cells for tissue remodeling. Stem Cells 30:2498–2511.

102. Kim Y, MI Fiel, E Albanis, HI Chou, W Zhang, G Khitrov and SL Friedman. (2012). Anti-fibrotic activity and enhanced interleukin-6 production by hepatic stellate cells in response to imatinib mesylate. Liver Int 32:1008–1017.

103. Biswas S, TL Criswell, SE Wang and CL Arteaga. (2006). Inhibition of transforming growth factor-β signaling in human cancer: targeting a tumor suppressor network as a therapeutic strategy. Clin Cancer Res 12:4142–4146.

104. Gotzmann J, A Fischer, M Zojer, M Mikula, V Proell, H Huber, M Jechlinger, T Waerner, A Weith and H Beug. (2006). A crucial function of PDGF in TGF-β-mediated cancer progression of hepatocytes. Oncogene 25:3170–3185.

105. Battegay EJ, EW Raines, RA Seifert, DF Bowen-Pope and R Ross. (1990). TGF-β induces bimodal proliferation of connective tissue cells via complex control of an autocrine PDGF loop. Cell 63:515–524.

106. Klass B, A Grobbelaar and K Rolfe. (2009). Transforming growth factor β1 signalling, wound healing and repair: a multifunctional cytokine with clinical implications for wound repair, a delicate balance. Postgrad Med J 85:9–14.

107. Zavadil J and EP Böttinger. (2005). TGF-β and epithelial-to-mesenchymal transitions. Oncogene 24:5764–5774.

Address correspondence to:
Prof. Michelle R. Dawson
Georgia Institute of Technology
School of Chemical and Biomolecular Engineering
311 Ferst Drive, NW
Atlanta, GA 30332-0100

E-mail: mdawson@gatech.edu